

UNCLASSIFIED

AD NUMBER

ADB232975

NEW LIMITATION CHANGE

TO

Approved for public release, distribution
unlimited

FROM

Distribution authorized to DoD only;
Specific Authority; Jan 98. Other requests
shall be referred to US Army Medical
Research and Materiel Comd., ATTN:
MCMR-RMI-S. Fort Detrick, MD 21702-5012.

AUTHORITY

USAMRMC ltr dtd 21 Jan 2000

THIS PAGE IS UNCLASSIFIED

AD _____

CONTRACT NUMBER: DAMD17-95-C-5040

TITLE: Non-Invasive Oxygenation Measurements in Surface and Deep Tissues

PRINCIPAL INVESTIGATOR: William Hayden Smith

CONTRACTING ORGANIZATION: MEDECO Company
Clayton, Missouri 63105

REPORT DATE: October 1995

TYPE OF REPORT: Final, Phase I

PREPARED FOR: U.S. Army Medical Research and Materiel Command
Fort Detrick, Maryland 21702-5012

DISTRIBUTION STATEMENT: Distribution authorized to DoD Components only, Specific Authority. Other requests shall be referred to the Commander, U.S. Army Medical Research and Materiel Command, ATTN: MCMR-RMI-S, Fort Detrick, MD 21702-5012

The views, opinions and/or findings contained in this report are those of the author(s) and should not be construed as an official Department of the Army position, policy or decision unless so designated by other documentation.

DTIC QUALITY INSPECTED 3

REPORT DOCUMENTATION PAGE

Form Approved
OMB No. 0704-0188

Public reporting burden for this collection of information is estimated to average 1 hour per response, including the time for reviewing instructions, searching existing data sources, gathering and maintaining the data needed, and completing and reviewing the collection of information. Send comments regarding this burden estimate or any other aspect of this collection of information, including suggestions for reducing this burden, to Washington Headquarters Services, Directorate for Information Operations and Reports, 1215 Jefferson Davis Highway, Suite 1204, Arlington, VA 22202-4302, and to the Office of Management and Budget, Paperwork Reduction Project (0704-0188), Washington, DC 20503.

1. AGENCY USE ONLY (Leave blank)	2. REPORT DATE	3. REPORT TYPE AND DATES COVERED
	October 1995	Final, Phase I 15 Mar 95 - 14 Sep 95
4. TITLE AND SUBTITLE		5. FUNDING NUMBERS
Non-Invasive Oxygenation Measurements in Surface and Deep Tissues		DAMD17-95-C-5040
6. AUTHOR(S)		
William Hayden Smith		
7. PERFORMING ORGANIZATION NAME(S) AND ADDRESS(ES)		8. PERFORMING ORGANIZATION REPORT NUMBER
MEDECO Company Clayton, Missouri 63105		
9. SPONSORING/MONITORING AGENCY NAME(S) AND ADDRESS(ES)		10. SPONSORING/MONITORING AGENCY REPORT NUMBER
U.S. Army Medical Research and Materiel Command Fort Detrick, Maryland 21702-5012		

11. SUPPLEMENTARY NOTES

19980127 063

12a. DISTRIBUTION / AVAILABILITY STATEMENT	12b. DISTRIBUTION CODE
Distribution authorized to DoD components only, Specific authority. Other requests shall be referred to the Commander, U.S. Army Medical Research and Materiel Command, ATTN: MCMR-RMI-S, Fort Detrick, MD 21702-5012	
13. ABSTRACT (Maximum 200 words)	
MEDECO has demonstrated the proposed capabilities of MED-DASI (Medical-Digital Array Scanned Interferometer) as an oxygenation sensor for deep tissues. We have obtained higher S/N spectra over a broader spectral range in a shorter integration period through a greater depth of tissue than any reported literature spectra. We have obtained hyperspectral oxygenation measurements. We find that spatial information from deep tissues survives and define methods for its retrieval via its spectral content. Typical MED-DASI parameters, as used in these tests, are: Penetration Depth: over 50 mm at 850 nm (flash lamp) ; Spectral Coverage: 600-1100 nm Spectral Resolution: over 200 ; Angular resolution: 1 milliradian (imaging) ; fiber determined for fiber coupling ; S/N: over 1000 per frame for integration under 1 sec. Size: test DASI: 1" diameter, 3" length, (without detector/interface) ; Weight: 3 oz. Temperature range: ±40°C ; Computer: 486x66 equivalent ; Power: battery capable These capabilities are realized in rugged, small, low weight and power sensors that are insensitive to ambient conditions such light variability, vibration, temperature variability, etc. Hence, the feasibility of a field-capable sensor to measure oxygenation in deep tissues is demonstrated.	

14. SUBJECT TERMS		15. NUMBER OF PAGES	
hyperspectra interferometry oxygenation of tissues		37	
16. PRICE CODE			
17. SECURITY CLASSIFICATION OF REPORT	18. SECURITY CLASSIFICATION OF THIS PAGE	19. SECURITY CLASSIFICATION OF ABSTRACT	20. LIMITATION OF ABSTRACT
Unclassified	Unclassified	Unclassified	limited

FOREWORD

Opinions, interpretations, conclusions and recommendations are those of the author and are not necessarily endorsed by the US Army.

N/A Where copyrighted material is quoted, permission has been obtained to use such material.

N/A Where material from documents designated for limited distribution is quoted, permission has been obtained to use the material.

N/A Citations of commercial organizations and trade names in this report do not constitute an official Department of Army endorsement or approval of the products or services of these organizations.

N/A In conducting research using animals, the investigator(s) adhered to the "Guide for the Care and Use of Laboratory Animals," prepared by the Committee on Care and Use of Laboratory Animals of the Institute of Laboratory Resources, National Research Council (NIH Publication No. 86-23, Revised 1985).

N/A For the protection of human subjects, the investigator(s) adhered to policies of applicable Federal Law 45 CFR 46.

N/A In conducting research utilizing recombinant DNA technology, the investigator(s) adhered to current guidelines promulgated by the National Institutes of Health.

N/A In the conduct of research utilizing recombinant DNA, the investigator(s) adhered to the NIH Guidelines for Research Involving Recombinant DNA Molecules.

N/A In the conduct of research involving hazardous organisms, the investigator(s) adhered to the CDC-NIH Guide for Biosafety in Microbiological and Biomedical Laboratories.

Wm Hayden Drury 10-14-95

PI - Signature Date

TABLE OF CONTENTS

ABSTRACT	PAGE 2
INTRODUCTION	PAGE 3
PHASE I RESULTS	PAGE 4
CONCLUSIONS	PAGE 14
INSTRUMENT SPECIFICATIONS	PAGE 14
REFERENCES	PAGE 18
APPENDIX A	PAGE 20

**MEDECO PROPRIETARY INFORMATION CONTAINED ON
PAGE 6 AND PAGES 10-17 INCLUSIVE**

INTRODUCTION AND BACKGROUND

Measurement of oxygenation levels via pulse oximetry has become an important medical diagnostic. However, an accurate, sensitive, inexpensive monitor for oxygenation of surface and deep tissues (e.g. the liver or the cerebrum) is not presently available when simultaneous, spatially resolved data or depth resolution is required. Such monitors are required for situations or circumstances where an individual has been or is being subjected to trauma. Accurate measurement of oxygenation of various tissues is a key status determining element in cerebral or other tissue hemodynamics and energy metabolism and thus, in the continuing viability of the patient.

A non-invasive, rapid, accurate determination of blood oxygenation, blood volume and flow for organs or tissues that have been subjected to trauma, environmental stress, or disease is an high priority requirement for determination of patient life status. An inexpensive, field capable sensor would match the Army's requirement to measure oxygenation levels in casualties to maintain them via appropriate intervention during transport to hospital facilities.

Hemodynamics and metabolism may be determined accurately via positron emission tomography. This is, however, a costly, cumbersome process. Nuclear magnetic resonance spectroscopy, NMR, recently developed for similar applications, suffers from accuracy as well as differentiation problems, requires the infusion of large amounts of ^{13}C glucose and, like PET, is cumbersome, slow, and expensive. Both PET and NMR are accomplished with physically large sensors that can be used only in permanent installations and are inconsistent with field portable operation.

Near infrared (NIR) spectroscopy offers a non-invasive, yet potentially quantitative blood oxygenation and volume/flow measurement technique (see Wyatt et al.(1990), Edwards et al.(1988), Maitland et al.,(1993), Ertefai and Profio (1985), and Arakaki and Burns (1992) among many such studies). The full potential of this method has, however, not been realized. Further, a sensor that is compact, portable, and self-powered for real time monitoring of the above patient variables, particularly with spatial information, has not been available, but such a sensor offers significant value when achieved.

There are significant barriers to the achievement of the stated measurement goals. Among these barriers are the high extinction of light incident upon the human body both in scattering and absorption processes, the nature of the volume scattering encountered by emergent photons, the complexity and (time) variability of the components of the blood and the intervening tissues, and patient safety issues such as limiting the incident flux of light even of relatively innocuous wavelengths. Physical measurement limitations include sensor *etendue* and efficiency, the statistics of detection, sensor calibration and mathematical diagnostic methods. Finally, the achievement of the desired measurement goals must finally result in the development of a low cost, low weight sensor ruggedized for field use. This report describes proof-of-concept data demonstrating that a portable field monitor is attainable.

MEDECO, Inc. intends to fabricate field portable oxygenation sensors with spatial resolution capabilities. The addition of spatial information adds an important dimension to the analysis. This sensor is based upon our patented Digital Array Scanned Interferometer, hereafter, the MED-DASI. The MED-DASI report is in two parts. Part 1 describes the design of the sensor and Part 2 describes the required development of quantitative analytical methods of hyperspectral data interpretation that permit rapid casualty evaluations for essential life-sustaining intervention under field conditions. The sensor fabrication and the operational software for field operation are specified.

PHASE I RESULTS

1. An Example MED-DASI NIR Spectrum:

The prototype MED-DASI we have developed for our Phase I research has demonstrated more than sufficient sensitivity in the NIR (600-1100 nm) and in the SWIR (850-2500 nm) to detect and image tissues via the presence of oxygenated and deoxygenated forms of hemoglobin, myoglobin, and cytochrome (HMC, hereafter). An example DASI spectrum is shown in Figure 1. This spectrum was obtained at a S/N of several thousand in a short observation time and exhibits strong spectral contrast including well known hemoglobin and myoglobin features. Cytochrome spectral features are also certainly present, however, the existing laboratory spectra are not believed adequate (Wray et al.(1988)) to define the expected, *in vivo* spectrum, so we only note the anticipated spectral positions. This spectrum covers a broad spectral region at high S/N with simultaneous spatial resolution for tissues at a depth greater than 30 mm. In an examination of the literature, I have not located any spectra of comparable quality, none that observed in transmission at the depth attained easily with the DASI, and none that purported to provide simultaneous spatial information at multiple sites. The ability to acquire H_2O spectral features at the same time provides an internal reference standard for the **quantitative** calibration of the spectral data (as is under development in a number of laboratory programs, e.g. Elwell et al, 1991).

The attainment of high S/N over a broad spectral region is an essential component of an accurate, reliable field instrument, as will be discussed in later sections in detail.

2. Spectral Region of Interest:

In order to define more precisely the spectral region of greatest interest, the literature was first surveyed. Graaf et al. (1993), Marchesini et al. (1989) and particularly Maitland et al. in gall bladder studies, and Parsa et al. (1989) who studied rat liver optical properties between 350 and 2200 nm show data that support the idea that substantial light transmission through useful, actual tissue paths is found only between about 600 nm and 1250 nm.

Our prototype MED-DATA measurements in this spectral region show that detailed

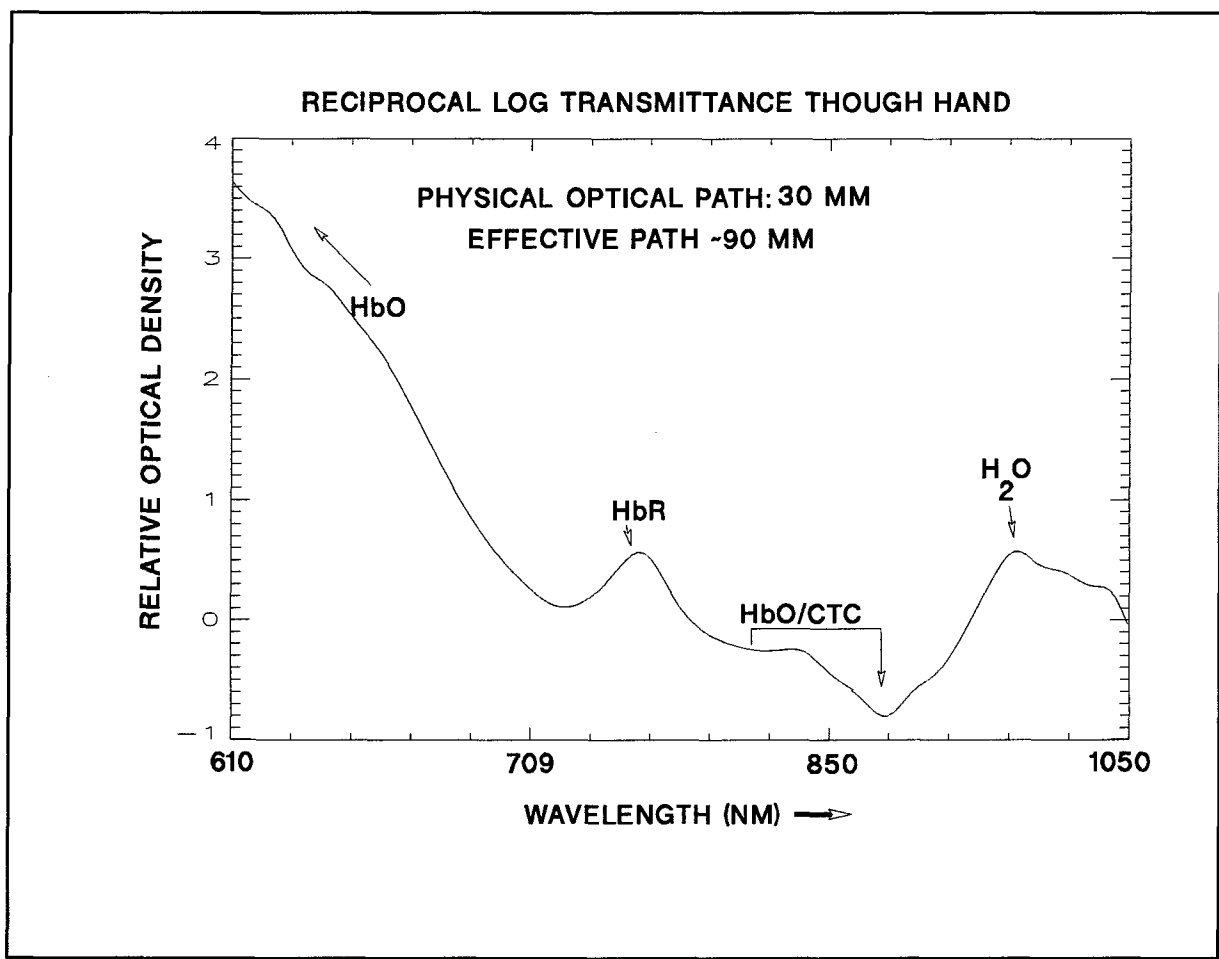


Figure 1. High S/N transmission spectrum of the human hand from 610 to 1050 nm showing a strong spectral contrast essential to oxygenation evaluations.

and spectrally rich features are readily detected through human bone and tissue approaching 50 mm thick. Our measurements show that SWIR light (1100 to 2500 nm) has an increasingly limited penetration depth beyond about 1200 nm in human tissues, eventually reaching depths of only a few millimeters. Visible light shorter than about 600 nm is highly attenuated in similar small depths. Thus, the primary spectral bandwidth for non-invasive NIR studies covers 600-1100 nm. Deleting the 1100-1250 nm region is dictated by detector (price, type) considerations although developments in array detector technology is reducing the price for arrays that operate beyond 1250 nm. Given a Ge or InGaAs array at a low enough price, the full spectral region would be accessible.

The entire concept of NIR non-invasive measurement of blood oxygenation, then, relies upon the efficient introduction and collection of light in that spectral region at the highest possible signal-to-noise, followed by analytical processing to yield real time measurement of the desired parameters; blood oxygenation, volume, and flow rate, spatially resolved, for the organs or appendages requiring diagnosis.

3. Light Sources for non-invasive NIR measurements:

Most of our measurements have emphasized battery powered flashlamps or cw tungsten-halogen lamps. These light sources are readily available, low cost and portable. These light sources are, however, not efficient in the context of the MED-DASI requirements since much of their output energy is at wavelengths of little interest, either visible or longer wavelength infrared. Hence, although these are viable sources of light, more efficient sources are available.

The MED-DASI prototype measurements provide reason to believe that the commercially available diode light sources are highly desirable for these measurements since:

- a. full spectral coverage is feasible with light-emitting diodes (LEDS) between about 600 and 1100 nm (the CCD response range) and further to 1250 nm.
- b. LEDs are highly efficient, produce little heat, no short wavelength radiation, have a directional output, and are easily modulated.
- c. LEDs are rugged, long-lived, and well suited to field operation and battery operation.

As result, an array (light bar) of LEDs is viewed as the optimal light source for the MED-DASI. The acquisition of the necessary LEDs, formation into a light bar, and coupling to receptor patches will permit illumination of the specific areas for spatially resolved oxygenation measurements. This concept is diagrammed schematically in Fig.2.

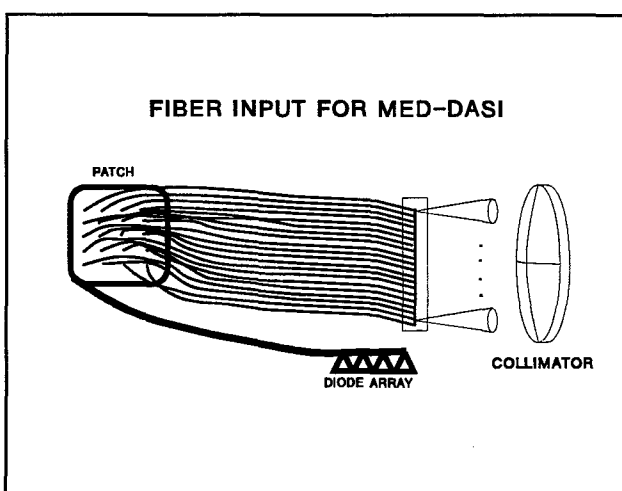


Figure 2. Fiber Optics can yield a light weight light source and collector that provides for area spatial resolution with MED-DASI.

CRITICAL DESIGN CRITERIA

The MED-DASI possesses specific instrumental parameters that yield substantial advantages in the present context of oxygenation measurements:

1. Etendue:

The etendue of an optical sensor is the product of the area of the spectral sorting element (e.g. a grating or a Wollaston prism) and the acceptance angle of the sensor at a given spectral resolving power. Thus, the larger the collecting area or the greater the angular acceptance of the sensor, the greater is the sensor's ability to deliver light to the detector. The

DASI is fully field widened and can accept any geometrically feasible light incident angle without loss of spectral resolution. This property allows the DASI to achieve much more than an order-of-magnitude increase in light acceptance compared with interference filters, grating monochromators, and interferometers that are not field-widened (Jacquinot, 1954). The gain in throughput from field-widening is critical in a small field instrument that necessarily has a small collecting area and fiber inputs.

The light received at the sensor after an incident flux passes through a substantial tissue path is diffuse and spatially extended. Thus, a large acceptance angle without loss of spectral resolution is a critical sensor characteristic in order to be able to collect the emergent, faint light. It is well known that most sensors are subject to the resolution-luminosity product limitation (also discussed by Jacquinot). This includes interference filters, grating spectrographs, scanning Michelson interferometer, but **NOT** the MED-DASI. This point is discussed in detail and experimental verification is given in our enclosed preprint (Smith and Hammer, Appendix A).

2. Sensor instrument function and spectral resolution.

Generally, a light sensor sorts photons before they are sensed at a detector, here a focal plane array (FPA). The sorting process relies on the sensor instrument function, a figure of merit description of the fidelity of the sorting process. The DASI, along with other two beam interferometers, possesses the optimum instrument function, the sinc function, (see Brault, 1985 for a lucid discussion of this concept). The effect of the optimum instrument function is that higher fidelity measurements can be achieved with less data, an important advantage for a field portable sensor.

3. Scattered and other light effects on the data.

The DASI is inherently insensitive to stray or scattered light in the sense that baseline drift caused by varying amounts of stray light does not contribute to the measured spectrum. This favorable property is valuable in a field sensor where conditions will generally be less than perfect and is a sharp contrast to an interference filter or dispersion-based sensor where any stray light reaching the detector is indistinguishable from the desired light. The result is that a DASI can yield a more accurate and quantitative spectral response since baseline offsets do not occur. This type of error is often referred in the literature as an accuracy limiting systematic error for dispersion sensors. Thus, unlike a sensor that uses an interference filter, grating, or other dispersion method, environmental light does not compromise the oxygenation measurement for a DASI as long as the detector is not saturated.

4. Efficiency.

The DASI utilizes components that are highly efficient throughout the required spectral region; as will any modern sensor. The DASI distinguishes itself, however, in maintaining a constant efficiency across the entire region (excepting detector quantum

efficiency variations which are common to all sensors utilizing the same FPAs.) For example, a grating has a blaze wavelength variation response that varies by more than a factor of two across the indicated spectral region. Interference filters have high efficiency at a peak wavelength, but their overall passband shape must be taken into account in the efficiency factor. Since filters allow only a few wavelengths to be sampled sequentially, the filter passband shape has a large effect on the interpretation of the data.

5. Simplicity, weight, and other physical criteria.

The MED-DASI is a solid state sensor with no moving parts. The prototype sensor is physically very small, weighing a few ounces (see Figure 3 for a photo of the prototype sensor). The electronics and fiber optics will yield a weight for a prototype sensor that is under 5 lb, most of which is due to the electronics package. The development of application specific electronics for the MED-DASI sensor could dramatically reduce the sensor weight, probably to well under one pound.

An important goal has been to retain the desired sensitivity and low cost, portability and reliability of the MED-DASI oxygenation sensor. A field capable MED-DASI design needs to be battery powered and capable of flexible operation for oxygenation measurements. That is, the same basic sensor should be fittable with different sensor heads, either contact or remote hyperspectral measurements. MED-DASI's characteristics for tissue oxygenation measurement include the capability for an high S/N determination and quantification of MHC oxygenation states due to the wide spectral and high sensitivity range attained.

Comparison with Older Technologies:

Pulse oximeters are used in areas of the body which are thin; the thumb or the ear lobe. The pulse oximeter is limited in selectivity by its two spectral point correlation. Commercial pulse oximeters are too large and complex for easy field use, although designs could certainly be reduced in size and ruggedized. The Hammamatsu NIR sensor (NIRO 500) improves on the pulse oximeter by providing a better, more stable parametrization. The Hammamatsu sensor is, however, slow, bulky, sensitive to patient and/or optode motion and subject to saturation due to its use of photomultipliers. The acquisition of spatial information would be a tedious point-by-point process with the Hammatsu sensor. The attainable spatial resolution is limited by the large fiber coupler optodes. In terms of sensitivity, the NIRO 500 cannot compete with the DASI since its detection scheme is not photon counting and does not remotely approach the photon noise limit attained by the DASI.

The MED-DASI also offers large throughput gains over traditional spectroscopic sensors for sensitive, non-invasive NIR spectral measurement and monitoring of HMC oxygenation states in diverse tissues. MEDECO's tests of aspects of the sensor permit specification of the MED-DASI capabilities. Hence, for the low light level measurements

inherent in transmission through substantial lengths of human tissue, the DASI has a demonstrable advantage in sensitivity due to its combined properties.

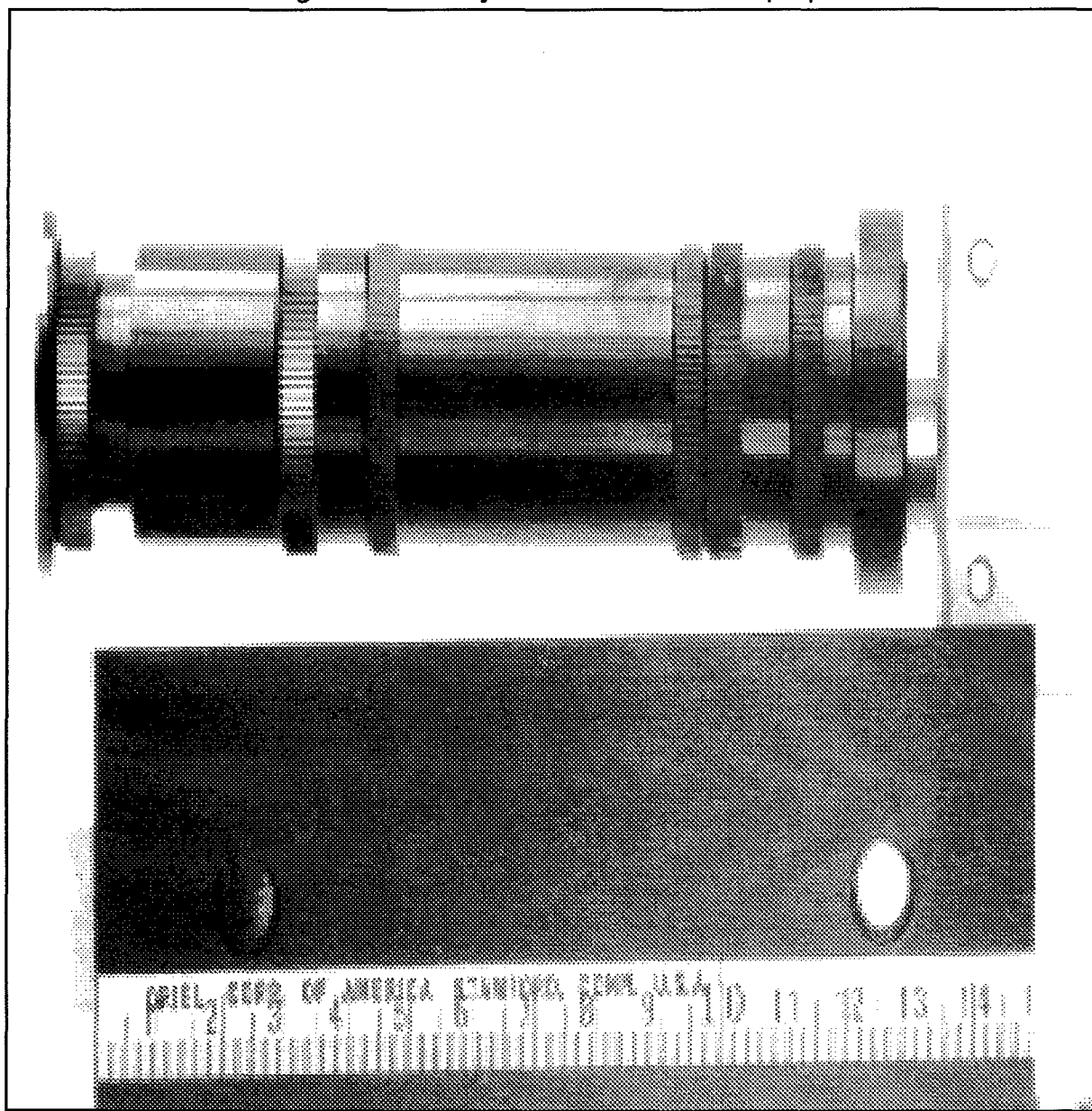


Figure 3. Photograph of a prototype MED-DASI with centimeter ruler for scale.

The prototype DASI, shown in Figure 3, is small enough for use on individual soldiers as a part of their personal equipment or for integration into proposed Army life support and transportation vehicles (e.g. LSTAT), unlike prior sensors. The MED-DASI is to be designed for battery operation and for simultaneous multi-point measurements using multiple receptor patches attached at strategic points. Thus, the MED-DASI will be

capable of imaging (mapping) the human body via simultaneous point measurements of oxygenation at multiple sites on the patient's body under field conditions. The MED-DASI detects a broader spectral range than previously reported in direct transmission measurements and, below, is amenable to fast/accurate methods of inversion of the measured DASI response.

The measurements we have obtained between 0.4 and 2.2 microns define a clear situation for the application of MED-DASI to oxygenation measurements. Therefore, adequate levels of light can be transmitted through the appendages and the cranium of adults for rapid, high signal-to-noise determination of blood oxygenation in the NIR (600-1100 nm). The other spectral regions can still yield useful, corollary imaging information, e.g. the calibration of the quantitative MED-DASI response. These regions can yield information on wavelength dependent scattering and absorption mean free paths that are needed in quantitative specification of the required blood oxygenation status. These data would be acquired simultaneously, forming part of the constraints on the model analysis.

Taken together, the experimental and theoretical analysis performed under Phase I has defined a flexible sensor that is readily fabricated. The MED-DASI, as evolved under Phase I, is a key to the verification and quantification of oxygenation measurement capabilities. It can serve in both a field and research application role.

THE HYPERSPECTRAL IMAGING POTENTIAL

We have obtained imaging data between 0.4 μm and 2.2 μm (see Figure 4) with the prototype MED-DASI. Our goal was to demonstrate spectral imaging with MED-DASI, the usefulness of specific spectral regions, and their penetration capability for human tissue. The results of the latter experiments have been summarized above. Imaging in back scattered (reflected) light has relatively few impediments and is a direct extension of oxygenation measurements previously done point by point. The illumination penetrates the body and is back-scattered towards the sensor, carrying with it the desired information on the tissues penetrated. The penetration depth is controlled by both absorption and scattering processes, as described above, a parameter which conveys important hyperspectral information.

Hyperspectral imaging in transmitted light may be more readily interpretable than backscattered (reflected) light since the emergent photons have transited all intervening tissue once. Single point measurement of transmitted light for spectral determination has been reported for small animals (e.g. Ferrari et al. (1989), and in infants and adults (e.g. Wyatt et al. (1990)). Multispectral imaging has been accomplished via short pulse time-of-flight measurements, but only in small animals (e.g. Benaron and Stevenson, 1993). Highly scattering human tissue obscures the origin of the transmitted photons and greatly attenuates their intensity. Quantitative analysis has been indirect, but shown reasonable accuracy compared with PET scans and other methods. Numerous, more or less

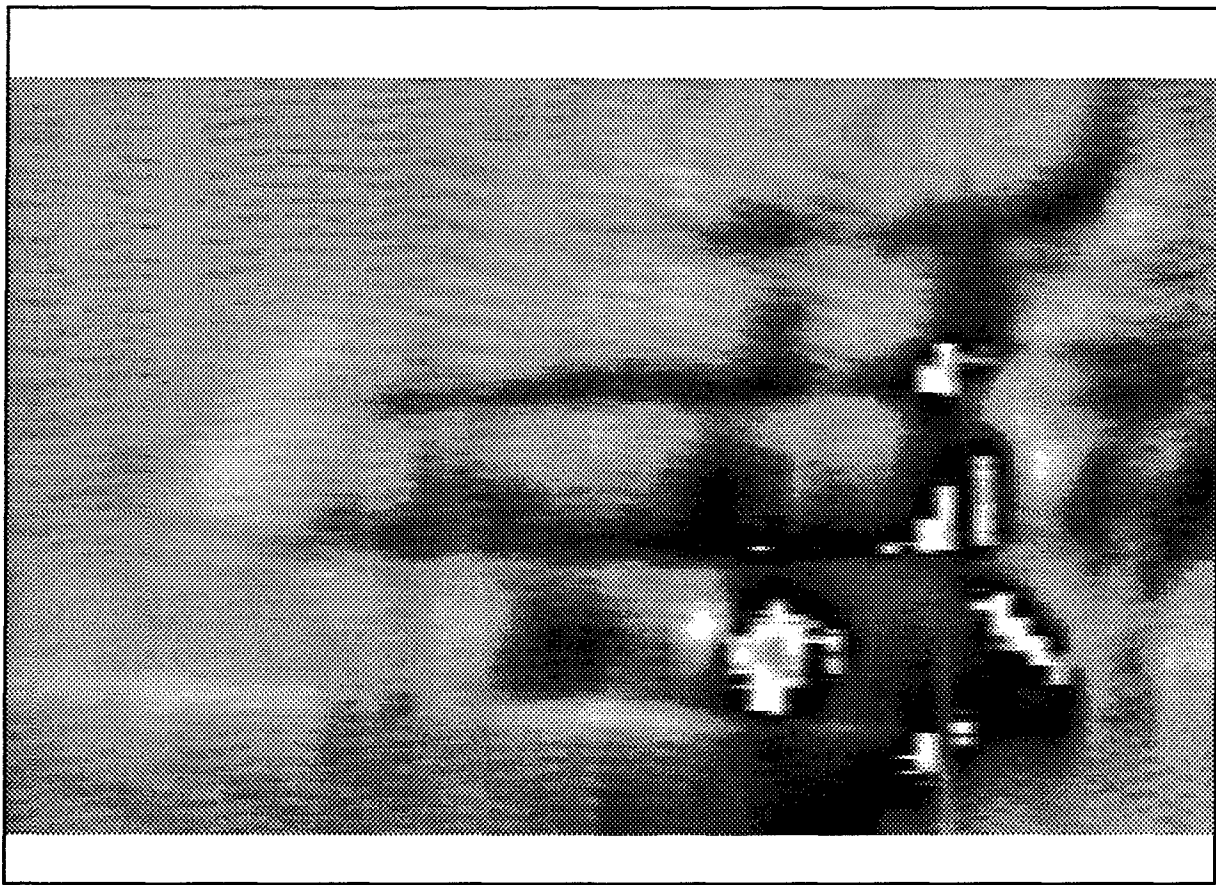


Figure 4. MED-DASI image of hand in SWIR reflected light. The bright areas are glints that result from point illumination.

classical, radiative transfer methods have been applied to the problem of light transfer through absorbing, scattering human tissue (e.g. Profio (1989)). These have been moderately successful, but are cumbersome, and at the moment, far too computationally intensive for routine analysis. Nonetheless, radiative transfer methods eventually offer the means for accurate interpretation of oxygenation sensor hyperspectra. As computers speeds advance, this situation will improve rapidly.

Since the extensive computation required by most approaches to the transport of light in human tissues presently exceeds the computational power of the envisioned MED-DASI sensor, we have sought a method to reduce these computations to the desktop and/or laptop pc level and have investigated alternate routes to the desired parameters.

The problem of isolating the measurements for individual organs other than the brain (since it can be accessed by direct transmission), particularly deep organs such as the liver, is challenging. However, the data acquired with the prototype MED-DASI to date suggest that high S/N hyperspectra in transmitted or back-scattered light can provide a data base for the determination of oxygenation parameters for surface tissues and for

organs at substantial depths within the body (at least 50 mm). The problem is to do the analysis economically.

Foremost, the oxygenation analysis must be routine and reliable. We have identified a rapid processing means that satisfies both criteria. Since the spectra of the HMC under in vivo conditions may (probably do) vary from laboratory spectra, the optimum analytical method should derive its end members from the data itself rather than from an external data base. The number of end members is quite limited. Recent developments in filter vector methods are directly applicable to this problem. For example, Price (1994) and Bowles et al. (1995) have described analytical methods that lead to the definition of a vector basis that spans the space of the hyperspectra. Then, all the end members' spectra consistent with the data are extracted along with their spatial dependence. Specification of the origin of the end member is reduced to a subsequent cross-correlation with the sought components. In the field, the desired species' form a look-up table used for cross-correlation. The end members also define the in vivo spectrum of the definable components better than presently available data, hence should be exploited to develop the data base itself by iterative calculation. Experience with DASI data from complex natural scenes, comparable in complexity with hyperspectral imaging in the human body, have shown that high S/N hyperspectra with a few hundred spectral elements and a large number of spatial elements provide powerful constraints on the appropriate vector basis set. This method of analysis requires no Fourier transforms on the data. The analysis is easily done on a typical pc and is amenable to implementation on fast, small, low cost CPUs. This method can be developed and implemented under the auspices of a Phase II program.

Quantitative Estimation of Oxygenation Parameters

We have undertaken a literature search and have defined the nature of calibration problems for oxygenation sensors in general. The solutions to these problems appear tractable within the auspices of a Phase II program. The effort required is substantial and requires feedback with clinical measurements for verification.

The major barrier to the acquisition of quantitative oxygenation hyperspectra has been the unknown path length for the radiation received after scattering by human tissue. A number of researchers have already utilized, in part, an obvious solution to this issue. The human body, in its various components, contains defined amounts of water. The absorption coefficients for water are well known and can yield an accurate value for the effective pathlength traversed by the incident radiation. The relatively high spectral resolution achieved by the MED-DASI allows the optical depth to be sampled accurately by measurements at well-defined positions with respect to the water spectral features. These spectral positions measure specific information on the oxygenated and deoxygenated species and since each measurement is made at many spectrally and spatially resolved positions, multiple constraints are achieved.

The NIR H_2O absorptions can serve for pathlength calibrations by providing the means to specify the optical path by measurement of their absorption. These features are on linear portion of the curve of growth hence, even in scattering situations, their strength is directly related to the effective path length.

Procedurally, the HMC spectral extinction (once a reliable cytochrome spectrum is obtained) is measured across the entire spectral region and calibrated by the relationship with H_2O features of the same optical extinction (see the spectrum in Figure 1.). The assumption that the effective paths are the same for photons at the same wavelengths, irrespective of their origin, is generally valid. This allows the calibration of the method to an accuracy determined by the actual knowledge of the proportion of H_2O to tissue in the sampled volume. The dehydration of tissues can be obviated by the use of calibrant tissue regions that are chosen due to the distance from a wound or water loss can be calibrated by tissue type.

The comparison of features of HMC near the H_2O features also provides a means to sample depth. The competition among scattering, absorption controls the penetration depth. We can measure to depths of 50 or more mm into typical (muscle, bone, etc.) tissues. The weak NIR HMC features have a linear response as do the H_2O features, providing an accurate measure of blood volume in the measured tissues. Depth is found from the comparison of scattering in the tissues and the path length from comparison to H_2O absorption. The full spectroscopic measurement by MED-DASI covers many spectral features of diverse strengths and provides strong constraints on the analysis that improve accuracy and precision of the method beyond that attainable by a multispectral sensor (e.g. three colors like the Hammamatsu sensor). The division of the incident light into more spectral bins reduces the flux per pixel at the FPA, requiring compensation by use of the MED-DASI's greater throughput. Our analyses of hyperspectra for natural scenes, obtained with the MED-DASI, indicate that the leverage of broad spectral coverage along with the concomitant enhanced spectral contrast yields a large enhancement of sensor sensitivity above that attainable with few-color data even when lower S/N is attained per spectral resolution element.

Further, profile analysis will allow the separation of the contributing spectra at specific wave numbers. Then, known absorption coefficients permit direct interpretation of oxygenated and deoxygenated forms of HMC.

Blood flow is measured by detailed balance considerations, i.e. the inflow and outflow must ultimately be equal. Any change in blood flow or oxygenation then permits the reestablishment of equilibrium to be followed. The blood volume is estimated from the hemoglobin and myoglobin spectral features as calibrated by the H_2O features. Changes in blood volume also indicate blood flow change. Differential measurements may be extracted from the high temporal resolution MED-DASI data. Derivative behavior differs among the HMC species. We are presently extending our calculations from our present data on how to best to extract that information for the MED-DASI sensor.

CLINICAL VERIFICATION

Clinical verification is required for all aspects of the routine use of the MED-DASI sensor. For example, measurements under controlled conditions, such as grown, thin tissue samples and animal experiments, followed by clinical studies, are anticipated in collaboration with Children's Hospital, Washington University, Neonatal Critical Care Facility under Director, Dr. Julio Fontán. Due to the developments under Phase I reported herein, we now can demonstrate feasibility and can confidently pursue, jointly and separately, funding for this research that underpins the field and clinical applications intended for the MED-DASI.

CONCLUSIONS

The MED-DASI, as demonstrated above, has an ability to collect rapid, high S/N hyperspectral information for measurement of the oxygenation of HMC and the flow of blood in human tissues. The sensor capabilities have reached a sensitivity level that is determined only by physical and spectroscopic parameters of the observed system. Once such information is acquired by the sensor, it is then essential to extract the required information quickly and at low cost. The prototype sensor that is be developed by MEDECO utilizes cutting edge numerical analysis methods to achieve these goals. We plan to continue analysis of our prototype MED-DASI data from various regions of the body to conduct a calibration based on the simultaneously measured H_2O and HMC features. We expect to achieve a calibration based upon water spectral correlations and profile analysis, estimated good to within 20% by comparative tissue measurements.

FABRICATION OF THE MED-DASI

Detector Selection:

The spectral region of emphasis defines the optimum FPA to be the silicon CCD with high response between 600 and 1100 nm. The rapid acquisition of high S/N hyperspectra is an high priority. The image of the hand shown in Figure 3. was acquired in about 75 seconds at a rate of about one frame per second. This rate was limited by the pushbroom mode of data acquisition. The MED-DASI, using area receptors, will acquire multiple hyperspectra for a large number of areas on the body simultaneously at the rate of once per second. This data rate will easily allow monitoring of temporal oxygenation changes in the patient and the patient response to remediation and intervention. The sensor would permit the acquisition of high time resolution hyperspectra, the reduction of those data to the specified oxygenation parameters, and the display of the essential information in real time. Since the display mode will be hyperspectral images in planes isolated by the vector analysis, each image will be readily interpretable.

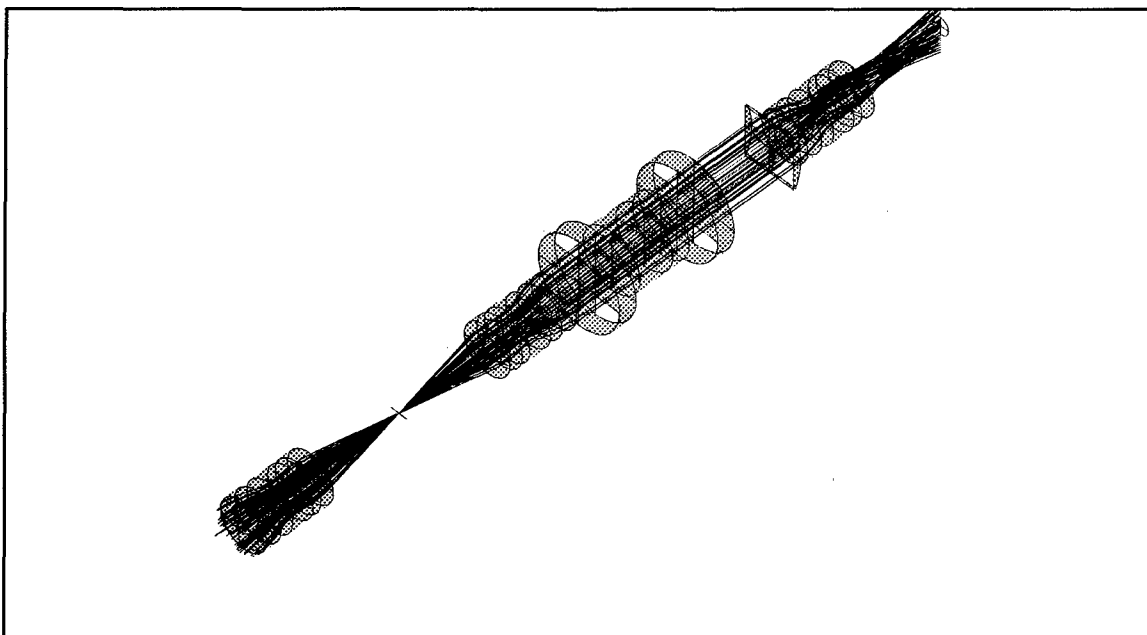


Figure 5. Optical ray trace for a MED-DASI design (near full size). The imaging element (lower left) is replaced by a fiber input for the contact area imaging mode.

Optics

The optics for MED-DASI will be fabricated after detailed optical calculation. A preliminary design, shown in Figure 5 at near full size, is suited for remote imaging. The fiber-optic coupled design to be fabricated will omit the telescope optics and replace them with fiber inputs as schematically shown in Figure 2. The use of multiple fiber inputs, placed side-by-side, will allow the MED-DASI to select electronically which and how many sites to monitor for a particular patient. The optical design for the fiber input mode will include the full optical path including the fiber receptors.

Fiber Receptors

The fiber receptor patches will be designed to place over or near areas requiring monitoring and to remain in place as long as required. Each patch will contain a fiber bundle illuminated with a fast wide angle gradient index lens. Both the fibers and the gradient index lenses are widely available types, as happily, the wavelength region of greatest interest to the MED-DASI is also the prime area for data and other communication systems utilizing fiber optics. Thus, highly efficient fibers and optics along with required A/R coatings are commercially available.

Light Emitting Diodes

The same commercial interests that have led to the desired fiber optics above have

motivated the development of light emitting diodes (LED) completely covering the wavelength range of interest, permitting the fabrication of an effectively continuous spectral coverage light source from LEDs. Such light sources are reliable, stable, and rugged. They are readily packaged with each receptor patch permitting the selection of when and which patches to activate for oxygenation measurements.

Electronic Interface and Data Analysis

The command and control of the FPA will be via the manufacturer's hardware in the prototype MED-DASI. That packaging is not be optimized for low size, weight, or power. The selected CCD electronics package will provide for the multiframe command mode we require. That interface will be modified to accept external control for synchronization with the LED pulsed operation.

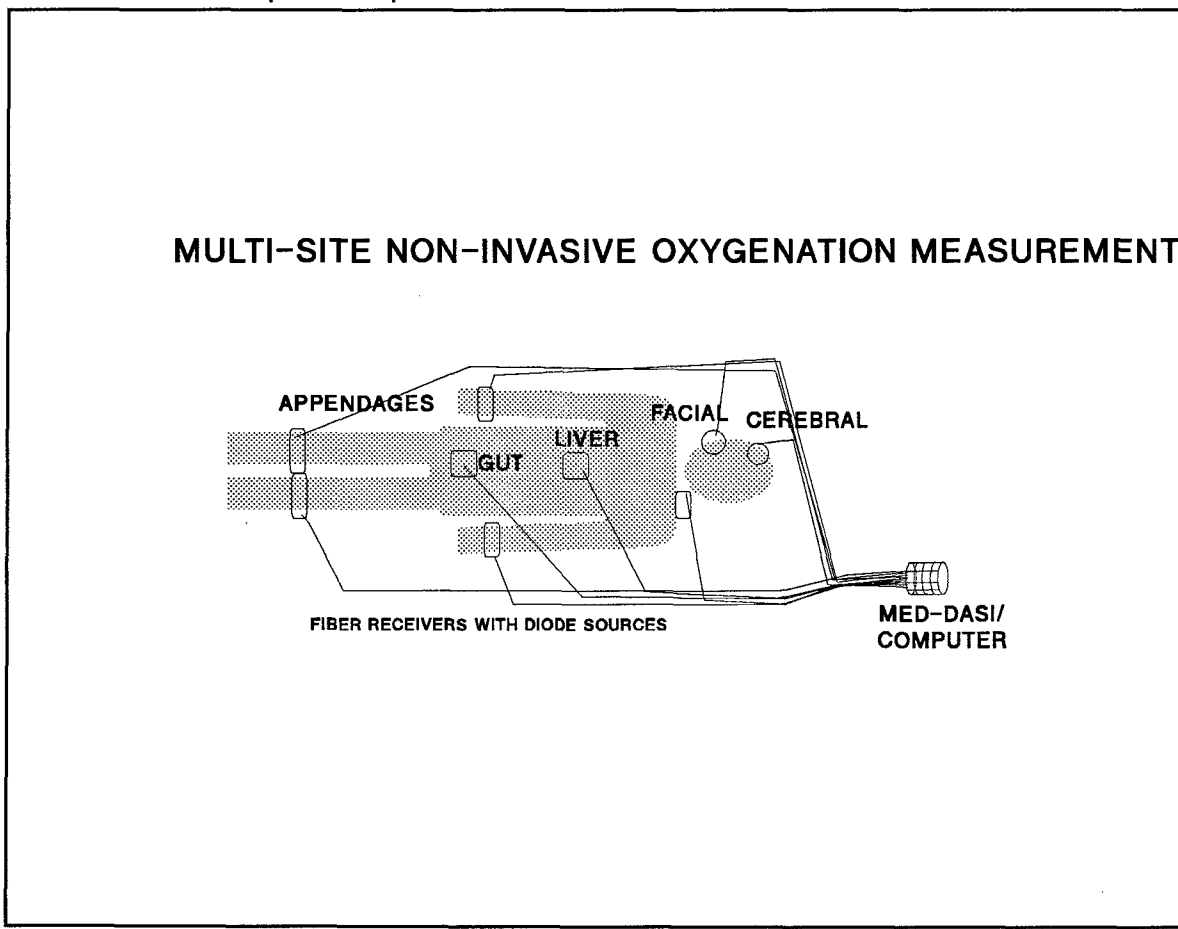


Figure 6. Fiber-coupled area multi-site oxygenation sensing with the MED-DASI.

The data acquisition and analysis (A&A) computer needs to be equivalent to or better than a 66 MHz 486. The data input will be either via a SCSI port or an enhanced

parallel port. This avoids the need for a frame grabber at additional cost and complexity. The laptop will be used to test reduced instruction set procedures for data A&A. The experience will be used to acquire a fast cpu using a minimum instruction set to carry out real time analysis of the MED-DASI hyperspectra.

Mechanical Components

The MED-DASI optics and FPA will be packaged in a lightweight package that is rugged and of low flammability. This package is expected to be small enough to carry at the belt. Initially, the computer will be separate. A successful minimum instruction set cpu development will enable the entire sensor to be packaged in a unitized package with a display readout. The MED-DASI will then be fully field capable for reading oxygenation at selected sites over the body in real time, as shown schematically in Figure 6.

Future Developments Suggested by this work

In the course of this research effort, we have realized that a number of improvements to the sensor and data analysis concepts are feasible. These, however, fall outside the sub-topic and hence are proposed for Phase II development. Without detailed discussion, we note those concepts here.

The hyperspectra acquired by the MED-DASI as developed for the sub-topic can also be obtained efficiently by remote observation, i.e. non-contact. That mode of operation results in a slightly more complex sensor as it is necessary to provide for the pushbroom imaging. This was done to acquire the data in Figure 4. The advantage of remote imaging is that an area may be worked on while making simultaneous oxygenation measurements. This has many obvious applications for surgery.

We have obtained preliminary measurements for a "tomographic-like" hyperspectra with the MED-DASI. This method allows an even greater sensitivity (read, penetration depth) to be achieved than the present imaging mode, but requires increased computational effort to achieve the enhancement. That level of computation is not feasible for a personal soldier field instrument, but could be used in field hospitals or during surgery.

Further means to solve the radiative transfer analysis problem have been investigated. Each approach has certain advantages, however, their implementation are beyond the means of a Phase I program. Among the methods which offer the greatest promise are:

1. Bayesian model-based probability analysis using the large measured parameter field determined by the MED-DASI. This method is non-linear but is known to converge rapidly and to yield an accurate probability assessment based on the model assumed.
2. Ray trace analysis of the hyperspectra. This method uses known parameters but is highly computationally intensive and beyond the capability of a field instrument at present.

Other methods are being developed that are promising for the complex, non-planar scattering problem encountered in human flesh. Although promising, none are as directly interpretable as the two approaches mentioned above. Our attentions will continue to be directed towards the evolution of the above methods,

REFERENCES

DASI and related references:

Smith, W. H. and W. V. Schempp, "Digital Array Scanned Interferometers", *Exp. Astron.* 1, 389-405, (1991).

Smith, W. H., U.S. Patent No. 4,976,542, (1990).

Smith, W.H. and Hammer, P.D., Digital Array Scanned Interferometers, Sensors and Results, *Applied Optics*, in press (1995).Appendix A.

Bracewell, R., " The Fourier Transform and Its Applications", McGraw- Hill, (1965).

Brault, J., Kitt Peak National Observatory, "High Resolution Astronomy", Proc. 15th Advanced Course in Astronomy and Astrophysics, SaaS-Fee, M. Huber,A. Benz, and M. Mayor, eds., 1985.

Hammer, P. D., D. L. Peterson, and W. H. Smith. "Imaging interferometry for terrestrial remote sensing - Digital Array Scanned Interferometer instrument developments". In: *Imaging Spectrometry*, SPIE Aerospace Symposium, Proc. SPIE 2480, in press,(1995).

Hammer, P. D., D. L. Peterson, and W. H. Smith. "An imaging interferometer for terrestrial remote sensing". In: *Imaging Spectrometry of the Terrestrial Environment*, Proc. SPIE 1937, 244-255,(1993).

Hammer, P. D. and W. H. Smith. "Spectral imaging of clouds using a digital array scanned interferometer", *Atmos.Res.*,34,347-366,(1994).

Jacquinot, P., "The Luminosity of Spectrometers with Prisms, Gratings, or Fabry-Perot Etalons", *J. Opt.Soc.Am.*,44, 761,(1954)

Clinical and Laboratory NIR Studies:

Arakaki, L. and Burns, D., *Appl'd Spectry*, 46,1919 (1992)

Benaron, D. and Stevenson, *Science*, 259, 1643 (1993).

Edwards, A., Richardson, C., et al., *The Lancet*, 4, 770, 1988.

Elwell, C.E., Cope, M., et al., *Proc. Cong. Int'l Soc. Oxygen Transport to Tissue*, 1991, preprint, 1992.

Ertefai,S. and Profio,A., *Med. Phys.*12, 393 (1985).

Ferrari, M., Wilson, D., et al., *J. Am. Physiol. Soc*, H1493 (1989)

Graaf, R., Dassel, A., et al., *Applied Optics*, 32, 435 (1993).

Maitland, D., Walsh, J., and Prystowsky,J., *Applied Optics*,32,586 (1993)

Marchesini,R., Andreola,S., Sichirollo,A., *Applied Optics*,28 (1989).

Nossal, R. Bonner, R., and Weiss, G., *Applied Optics*,28, 2238 (1989).

Parsa, P., Jacques,S. and Nishioka, N., *Applied Optics*,28, 2325 (1989).

Profio, A.E., *Applied Optics*, 28, 2216 (1989).

Tang, G., Sha,W., Liu,C., Alfano,R., Applied Optics,28, 2337 (1989).
Wyatt, J., Cope, M., et al., The Lancet, 2, 1086 (1990).
Wray, S., Cope, M., et al., Biochim.et Biophys. Acta,93, 184 (1988).

Image Restoration and Parameter Analysis:
Schulz, T. and Snyder, D., J.Opt.Soc.Am.9, 1286 (1992)

Imaging Tomography
Bernhardt, P. and Antoniades, J., S.P.I.E.,2480, 78 (1995).

Bayesian Estimates
Bretthorst, L., Bayesian Spectrum Analysis and Parameter Estimation, in "Lecture Notes in Statistics",48, Springer-Verlag, NY,NY.

End member and Band selection:
Bowles, J., Palmadesso,P., Rickard, L., S.P.I.E. Proceedings (1995)
Price, J.C., Applied Optics,15, 3281 (1994).

DIGITAL ARRAY SCANNED INTERFEROMETER:
SENSORS AND RESULTS

by

Wm. Hayden Smith
Department of Earth and Planetary Sciences
Washington University
St. Louis, MO 63130
and
MEDECO, Inc.
P.O. Box 207
New Melle, MO. 63365

and

Philip D. Hammer
Earth Science Division
NASA Ames Research Center
Moffett Field, CA. 94035

ABSTRACT

Digital Array Scanned Interferometers (DASI), blend characteristics of a grating spectrometer and a two-beam interferometer for acquisition of hyperspectra. DASIs possess field widened capabilities that permit very high throughput. Aspects of DASI design, hyperspectra and data processing methods are presented. In particular, we provide data showing that photon noise limited hyperspectra are achievable for DASI data.

APPLIED OPTICS, IN PRESS

INTRODUCTION

The Digital Array Scanned Interferometer, or DASI, is a new sensor, a stationary FTS that blends characteristics of the grating spectrometer and the scanning FTS. The DASI also adds new parameter choices not available to either of the other two sensors. Since there is no single "best" spectroscopic sensor for all possible spectroscopic measurements, the introduction of a new sensor with a different range of spectroscopic characteristics provides the potential to optimize the selected sensor for a wider range of tasks.

The principles behind the DASI are similar to those for other two beam interferometers. The emergence of the DASI at this time is mainly a result of the development of two-dimensional focal plane array detectors with an high quantum efficiency and a large linear dynamic range. Early efforts with a stationary FTS by Stroke and Funkhouser (1) yielded data of only modest signal-to-noise due to the limited dynamic range of film detectors. CCDs and other digital arrays have, in large part, relieved the dynamic range problem.

The most efficacious DASIs are those forms that are easily and stably aligned with fast, high throughput optics, and physically small dimensions. The SAGNAC or triangle path interferometer was studied by Yoshihara and Kitade (2) and shown to be quite stable due to its reentrant design. Another very useful form, the birefringent interferometer, was demonstrated by Okamoto et al. (3). This form has all the above desirable features. An heterodyned stationary interferometer utilizing a grating, the FRINGHE, has been developed by Douglas, Butcher, and Melis (4) to achieve high spectral resolution over a limited free spectral range. Although the FRINGHE is more difficult to align and operate stably than the DASIs discussed here, it provides the means to attain high

spectral resolution ($>100,000$) and high throughput in a small sensor, for example, to match very large telescopes' throughput.

The early demonstrations of stationary FTSs did not, however, realize their potential for spectral imaging, as described by Smith and Schempp (5). By resolving the spatial (redundant) dimension, the DASI is both multichannel (one spatial and the spectral dimension) and multiplex (the spectral domain) in operation. The realization of these concepts is embodied in a patent for the hyperspectra (imaging) aspects of DASIs (Smith, 6).

For an FTS (and a DASI), a multiplex disadvantage can arise in the photon noise limited case (see Kahn (7), Brault (8), and a further description below). The high throughput of DASIs and FTSs (9), their large free spectral range, lack of parasitic light problems, and the multichannel aspects of their data acquisition can largely compensate the multiplex disadvantage, given that high dynamic range FPsAs are available. The choice of an optimum sensor for a particular measurement goal requires a detailed consideration of the entire spectroscopic measurement system from the input spectrum to detected photons, as well as the rate of data acquisition.

DASI DESIGNS

Our recent development of DASIs has been based primarily on the birefringent DASI shown schematically in Figure 1. The birefringent DASI can be fabricated to provide high transmission and interference efficiency in the spectral region from $0.13 \mu\text{m}$ to beyond $11 \mu\text{m}$ using available birefringent materials (e.g. MgF_2 and HgS) and focal plane arrays. The long wavelength limit is due the present state of detector development (uncooled machined bolometers will extend this range soon).

BIREFRINGENT DASI

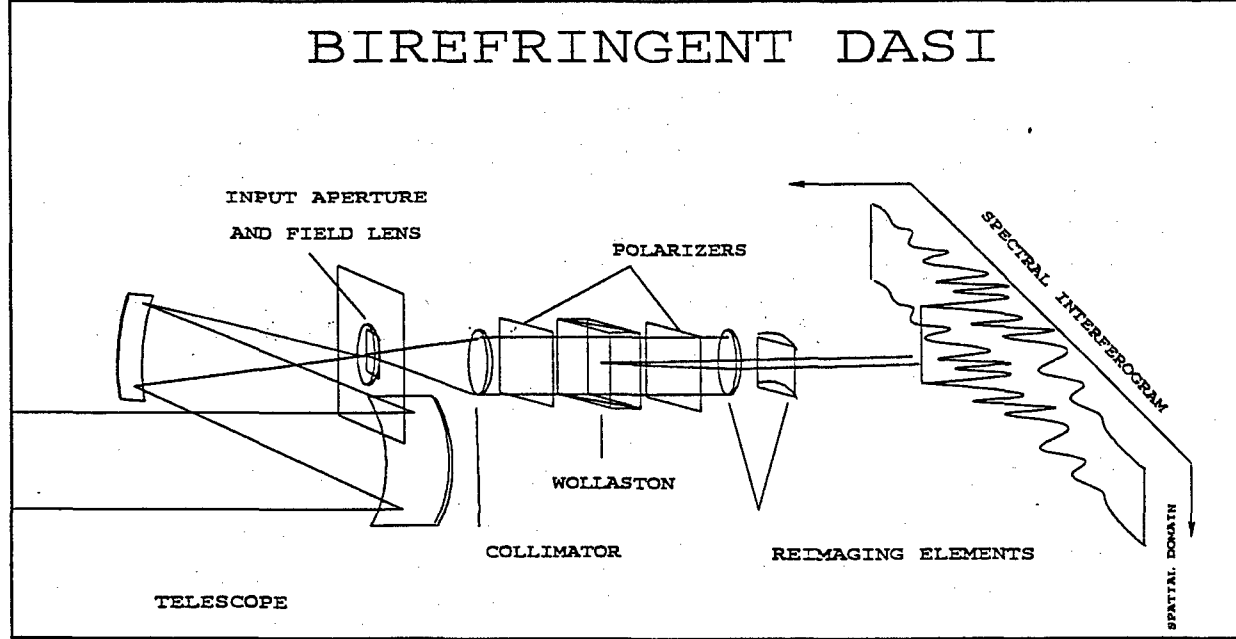


Figure 1. Schematic birefringent DASI illuminated with an off-axis telescope

Fresnel mirror DASI is an useful DASI form; efficient, compact, simple, and easily aligned. Although these designs can be efficient, they lack the throughput advantage of the birefringent and SAGNAC forms.

DASI hyperspectra require the simultaneous acquisition of a spatially displayed interferogram and one spatial dimension along the entrance aperture focussed simultaneously onto the FPA. This mode of data acquisition is the pushbroom mode where an entrance aperture is scanned across the scene to provide the second spatial dimension information.

Typically, in hyperspectral data acquisition, an IFOV ~1 mradian is desired. This large IFOV must be matched optically to the pixel size on a typical FPA. The IFOV (slit width or entrance aperture diameter) sets the spectral resolution for a dispersive sensor and an FTS. The DASI spatial and spectral resolution are set independently. Generally, we have found that this degree of freedom yields a consequent reduction of the size of the DASI compared with the other sensors for the same flux brought to the detector at a given spectral resolving power.

A small sensor size is an important consideration for mass constrained missions or for a portable field sensor. As a case in point, Smith (10) (in collaboration with Ball Aerospace) has designed and breadboarded a multispectral imager and a DASI for SWIR hyperspectra for a prospective Pluto mission where mass, power, and physical size are critical mission constraints. The resulting two sensor package, including a 10 cm aperture telescope, and supporting electronics massed less than 5 Kg with most of that mass in the electronics and telescope.

FTS THEORY AND DASIs

The theory of the FTS is clearly described in many sources (see Brault (8) for a comprehensive overview) and applies, with some modifications, to the DASI. In spite of their similarities, the DASI and the Michelson FTS may offer significantly different capabilities for hyperspectral studies due to their different mode of use of the FPAs.

-3-

SIGNAL DETECTION AND RECONSTRUCTION

The DASI, like an FTS, reconstructs only the ac portion of the incident signal, and thus responds to a dc background level only through its added noise contribution, limited by the dynamic range of the detector. As long as the detector is not saturated by the total incident signal, the DASI (and FTS) signal-to-noise is calculable directly from the incident flux and the sensor characteristics. This ac-only response is an important advantage of imaging two-beam interferometers compared with dispersive spectrometers or Fabry-Perot interferometers where a dc offset (e.g. from stray, parasitic, or scattered light) becomes indistinguishable from the desired signal. The ac-only response of the DASI also enables the formulation of effective algorithms for correcting systematic FPA and sensor defects.

Noise sources and their temporal characteristics have an, in principle, different effect for a DASI compared with an FTS. The DASI and the FTS, when equipped with the same FPA and illuminated with the same source with an equal field of view and aperture, can collect the same number of photons in the same time. Then, in principle, the attained S/N is the same. Due to the different mode of data acquisition, the DASI and FTS can yield a different S/N in the data in a given integration interval since the separate and various sources of noise may have different temporal, spatial, and wavenumber dependencies. In practice, the aperture of the FTS does not limit one dimension of the FOV, as for the DASI or dispersive sensors, so that a net gain in the rate at which flux reaches the FPA can be achieved in some cases. The utility of this gain depends upon the FPA duty cycle for integration compared with the frame rate.

THROUGHPUT AND STABILITY

The birefringent and SAGNAC DASIS are field-widened and can accept any geometrically feasible field of view without loss of contrast in the interferogram. Then, an object anywhere in the field of view produces the same spectral response. This property is demonstrated in Figs. 2-5 below. In addition, birefringent DASIS have an inherent alignment stability, easily yielding white light fringes. Field-widened FTSs have been achieved over limited wavelength ranges by introducing media with the required dispersion to counter off-axis frequency shifts inherent in the FTS. A scanning Michelson FTS is relatively unstable and alignment and location of the central fringe in white light is difficult. To achieve stability and proper sampling of the interferogram, an FTS scan is servo-controlled by an auxiliary laser to maintain mirror alignment and position. Of course, FTS scanning is a solved problem, but the moving mirror and laser reference can still introduce spectral artifacts and contribute to a more complex sensor than a DASI, with a susceptibility to external noise and laser induced spectral errors that do not occur for DASIs. On the other hand, the auxiliary laser of an FTS provides a precise means to determine the wavenumber of observation that is not available in the DASI in the same fashion.

OBSERVATIONAL SCANNING MODE OF DASIS and FTSs

An imaging FTS integrates a selected field of view and accumulates a multiplexed image at each of a time series of mirror positions that each yield one point on an interferogram for each spatial IFOV. The signal-to-noise in the FTS interferogram is limited by the degree of normalization of any variations in the incident flux during the acquisition of the time series interferogram. Even then, variable spectral content of the incident flux during acquisition can cause

-4-

spectral artifacts and S/N degradation. Hyperspectra are then formed from the series of multiplexed images.

The DASI field of view is typically scanned by moving the aperture across the FOV while acquiring the spectral and one spatial domain in a multichannel mode. A DASI scan mirror requires only that the angular motion resolve the angular IFOV. The motion should be repeatable to a small fraction of an angular IFOV for repeated scans. This requirement specifies the stability of the mounting platform rather than the DASI.

A DASI acquires data multichannel and multiplexed in wavenumber and multichannel in one spatial dimension while the FTS is multiplexed in wavenumber, but is not multichannel in the spectral domain. The two FTS multichannel dimensions are the spatial channels. For measurements emphasizing the spectral channel, the DASI would tend to reduce the effects of temporal noise which should improve "spectral correlation". Conversely, a measurement that requires the spatial domain to be measured simultaneously may be done more effectively with an FTS (or a Fabry-Perot Interferometer) since these are direct imaging devices. These facts imply that a measurement in which the spectral domain is the more important may be done with better results with a DASI while spatial information may be better correlated in data from an FTS. Direct comparisons that verify these implications are lacking and depend upon sensor effects such as FPA pixel-to-pixel variations and the algorithm used to effect a correction (see below).

DASI OBSERVATIONS

The independence of DASI interferograms (and spectra) on the field of view is demonstrated in Figures 2-5. Figure 2 is an interferogram

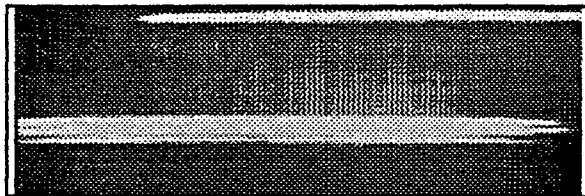


Figure 2. DASI interferogram of Orion around the Trapezium, showing the nebular emission.



Figure 3. Slitless DASI interferogram of a low brightness, starless Trapezium region.

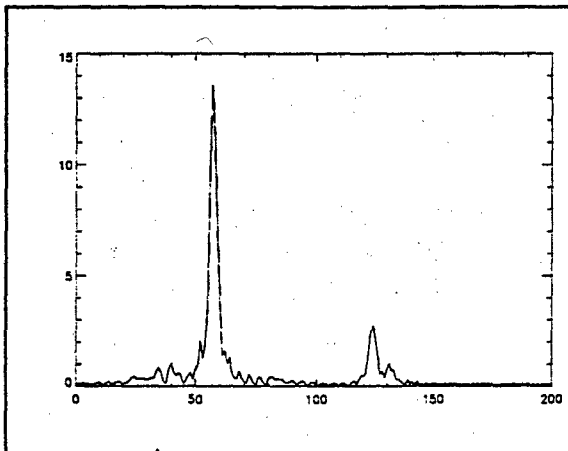


Figure 4. Spectrum of 100 averaged rows of the Trapezium nebulosity. The strong feature is $\text{H}\alpha$.

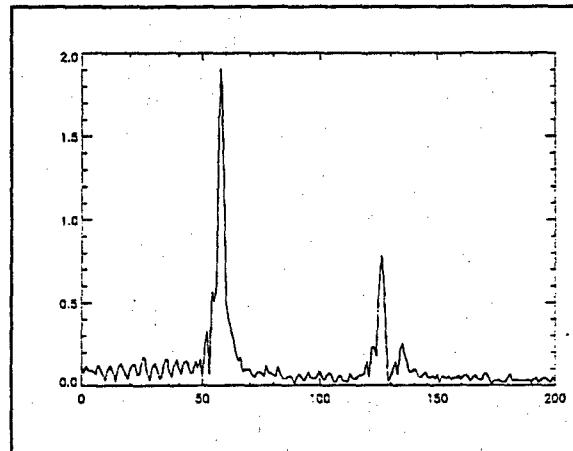


Figure 5. Spectrum from the slitless interferogram. The strong feature is $\text{H}\alpha$.

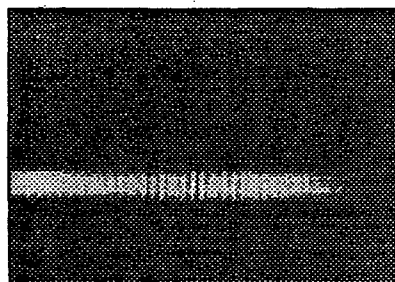


Figure 6. DASI interferogram image for Jupiter (1.2-2.2 μm)

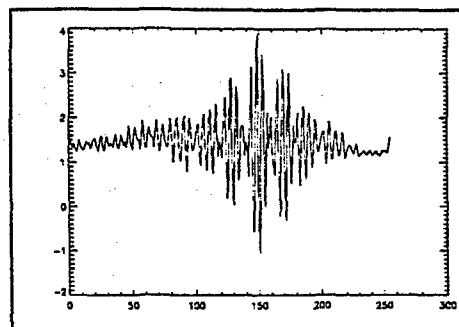


Figure 7. Trace of SWIR interferogram for Jupiter obtained with the DASI.

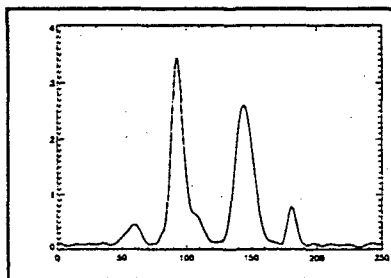


Figure 8. FFT of the Jupiter interferogram, showing the strong CH₄ features.

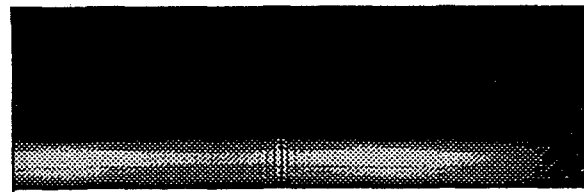


Figure 9. Jupiter visible-nir interferogram obtained at Mauna Kea with DASI.

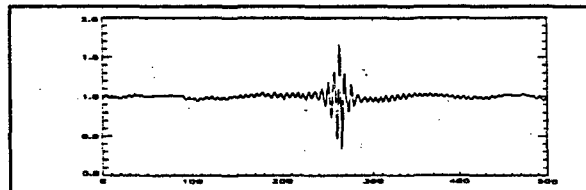


Figure 10. Center of disk DASI interferogram for Jupiter in the visible-nir.

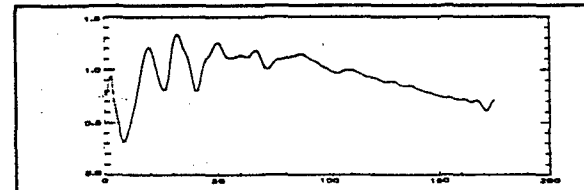


Figure 11. DASI FFT'd spectrum for Jupiter center of disk, visible-nir (right to left)

image of the Trapezium in the Orion Nebula, obtained with a 75 μm wide slit. The low bits of the image reveal the nebular emission underlying the Trapezium stars which are saturated at this level. Figure 3 is a corresponding interferogram image of a lower surface brightness region that had no obvious stars so that the slit could be removed (avoiding saturation of the CCD), yielding a 6 mm wide entrance aperture. The interferogram contrast is essentially the same in the two images although the latter image is exposed at a similar level in less than 1/30 the exposure time of the first. The Fourier transform of 100 rows of Figure 2 is plotted in Figure 4, while a single row of Figure 3 is transformed and plotted in Figure 5. The slightly smaller FWHM of the single row spectrum from the slitless example is a consequence of an imperfect alignment of the CCD with the optical axis. The contrast in the 100 row average from the interferogram in Figure 2 is reduced due to the summation of the rows. The DASI, thus, can achieve an high throughput at the expense of spatial resolution in one dimension without loss of spectral resolution.

Observations of Jupiter with a SWIR DASI have been obtained. Figure 6 is a DASI frame taken across the center of disk with a 1.2 -2.2 μm passband filter at a spectral resolution near 50. An trace of the interferogram near center of disk is plotted in Figure 7 and its FFT in Figure 8, showing the well known reflectance spectral absorptions of Jupiter due to strong CH_4 . The passband is limited by a 1.2-2.2 μm blocking filter which is not normalized here. The corresponding interferogram image for the Jupiter obtained with a CCD is shown in Figure 9, with the center of disk interferogram and FFT shown in Figures 10 and 11, respectively, again showing the anticipated visible-nir spectral profile for Jupiter at a spectral resolution of about 100. The same interferometer was used for both data acquisitions so that a dichroic beamsplitter at the exit

-5-

would have allowed both these images to be obtained simultaneously. The 0.61 m telescope on Mauna Kea, used to obtain these data cannot effect precise offsets. As a result, seven positions roughly evenly spaced across the disk were acquired for Jupiter. Similar, consistent data for Venus and Mars were also obtained.

DASI S/N Considerations

Here, we take a typical source to be broad-band with high light intensity levels. Many currently available focal plane arrays (FPA) can attain a photon shot noise limited response when electron wells for individual pixels are filled sufficiently to exceed the dark current and amplifier and read noise. So, when sensor parameters and integration times to reach these conditions can be selected, the photon shot limit can be achieved, in principle.

Under shot-noise limited conditions, Fourier transform sensors have a multiplex disadvantage that arises from the signal contributions of all the spectral components falling simultaneously on each pixel of an interferogram. The noise in a particular spectral channel of a Fourier transform sensor has contributions associated with the signals in all the other spectral channels, unlike dispersive sensors.

The attainable S/N can be written as a function of the flux reaching the detector within the allowed integration time, the spectral resolving power, the intensity distribution in the incident spectrum, the sensor function of the measuring sensor, the efficiency of its detection, and the sources of noise that degrade the S/N (see Brault (8) for a related discussion). Then, the interferogram domain (S/N) is defined as

$$(S/N)_i = (M/N)^{1/2}$$

where M is the total number of detected photons at the FPA and N is the number of spatial samples taken of the interferogram.

A DASI achieves S/N in the transformed spectrum $(S/N)_s$, compared with the measured interferogram $(S/N)_i$, defined as follows:

$$(S/N)_s / (S/N)_i = (B_t/BD) \times (N/2)^{-1/2}$$

B_t/BD is the ratio of the total spectral interval sampled from 0 cm^{-1} to $\sigma_{\text{max}} \text{ cm}^{-1}$, B_t , to the fraction of the spectral interval with spectral power, B , including the transmittance of the optics and the atmosphere or scatterers, etc. and multiplied D by the response function of the detector, all from 0 to $\sigma_{\text{max}} \text{ cm}^{-1}$. This result recognizes that the interferogram noise is redistributed by the Fourier transform evenly over the entire spectral interval (see Bracewell (11)), including the regions where we know no signal exists or where the array is not sensitive. $N/2$ is the number of observed spectral samples, divided by two to account for the half of the noise in the interferogram that goes with the imaginary part of the transform. $N/2$ is equal to the spectral resolution, R , for two-sided symmetrical sampling of the interferogram. In this equation, the S/N ratio in the transformed spectra and the S/N in the interferogram given by (1) has been compared with real data as follows.

For a dispersion spectrometer, the corresponding relationship is

$$S/N_\lambda = [F(\lambda) \delta\lambda]^{1/2} = [M(\delta\lambda)]^{1/2}$$

since each channel, $\delta\lambda$, collects M photons independently from the flux, $F(\lambda)$. These equations show that dispersion spectrometers, in principle,

-6-

may achieve an higher shot-noise limited S/N than DASIs for the same number of detected photons per unit spectral interval. In practice, it is essential to consider, for example, what is the resulting size and level of complexity of the dispersive spectrometer needed to achieve equal throughput (i.e. equal number of detected photons), what are the effects of FPA characteristics on the resulting S/N, and what performance limitations are caused by systematic errors and aberrations and as well, what wavelengths contain high flux levels? Due these effects, an higher S/N may not be achieved since the sensor parameters and calibrations may prevent dispersive sensors from achieving their theoretical signal-to-noise performance.

The throughput advantage and relaxed design constraints of DASIs compared with dispersive sensors address the issues of size and complexity, as we have already discussed in the referenced literature. Questions of systematic errors and aberrations are discussed below.

NOISE AND ABERRATION CAUSED BY FPA SPATIAL VARIABILITY

The signal-to-noise practically obtainable from any imaging spectrometer can be severely limited by defects and systematic irregularities in FPAs (i.e. non-responsive, unstable, and/or nonlinear pixels; drifting interpixel gain and offset variations). In addition to spurious noise, such imperfections can produce distortions and artifacts in the spectra. Numerical processing that overcomes detector imperfections to approach the theoretical signal-to-noise limit is clearly essential for all imaging spectrometers, but particularly for the DASI since its S/N is coupled directly to the degree of FPA correction. Generally, a two term

gain and offset correction is only a first approximation to the corrections required to reach photon noise limited operation (in these cases, also background-limited) operation of the FPAs, irrespective of the spectral device used.

The conventional "flat-field" calibration of an FPA uses an uniform intensity source to illuminate the FPA at differing brightness levels and/or integration times. These measurements are used to derive pixel gain and offset matrices to be used to correct spatially variable signals obtained during field measurements.

The calibration measurements should be made at about the same time and for the same optical and electronic configurations as the intended field measurements in order to minimize the effects of temporal drifts and other systematic errors. The measurement also corrects spurious focal plane array (FPA) signals that are proportional to the incident radiation signal (i.e. variations caused by stray light and defects in the optics). Generally, a uniform signal over the FPA may not be attainable even with a spatially uniform external target since structured patterns are always present for imaging spectrometers (spectra for dispersive sensors and interferograms for the DASI). Such structure, together with the difficulties in performing frequent calibrations in the field, tend to reduce the effectiveness of the conventional flat-fielding approach.

An Improved Algorithm for DASI Data Reduction

For the DASI sensor, we have formulated a series of algorithms that successfully treat FPA pixel-pixel effects by utilizing the properties of the spatial interferograms at the FPA. This has yielded a practical method for elimination of the systematic irregularities in DASI data. Illustrations of its application to observational data are presented here and were been described in detail by Hammer, Peterson, and Smith (12).

The overall objective of the calibration scheme is to achieve photon

-7-

shot noise limited signal-to-noise for a DASI image cube using information obtained from within that data sequence itself or from nearly simultaneous reference data. This capability is particularly important for field measurements where acquisition of reference data may not be practical, or for the treatment of data for which no reference is available. The algorithm described below accomplishes these goals and overcomes the calibration problems related to precise and accurate pixel-to-pixel and other systematic illumination effects. The DASI then yields interferograms and hyperspectra with a S/N at the photon noise limit. This result means that higher S/N in DASI hyperspectra can be achieved only by detecting a greater number of photons. The high throughput, field-widened DASI can increase of the level of incident photons without itself growing substantially larger so that increasing flux levels is feasible. These demonstrated capabilities are useful in many contexts.

It is advantageous to perform the calibration operation with the sensor optics assembled so that spurious focal plane array (FPA) signals that are proportional to the incident radiation signal may be treated as well (i.e. variations caused by stray light and defects in the optics). Under these conditions, a uniform signal over the FPA may not be attainable even with a spatially uniform external target. Structured pattern are always present for imaging spectrometers (for dispersive sensors, an FTS, and the DASI). Such structure together with the difficulties of performing frequent calibrations in the field reduce the effectiveness of the conventional flat-fielding approaches. A two term correction may be only a first approximation to the corrections required to reach photon noise limited operation (in the mid-ir or longwards this

is also background-limited operation) of the FPAs, irrespective of the spectral device used. The algorithm treats focal plane array (FPA) pixel-pixel noise effects by taking advantage of the physical properties of the DASI spatial interferograms. The approach begins with an interferogram frame constructed by coaddition of many raw data or reference frames. A prescribed series of reversible transformations to the two-dimensional Fourier domain of the array pixel space are then invoked. A key operation is a row-wise phase alignment algorithm, adapted from the formalism described by Forman et al. (13). Phase alignment eliminates the effects of variation in fringe path difference scales over the rows of the FPA. The essential result here is that the signal component in the Fourier domain becomes highly localized (Figure 12), enabling the effective separation of the systematic noise from the signal. The inverse composite transformation is then applied to the isolated systematic noise to yield a reference or pixel gain variation frame for subsequent treatment of individual raw data frames. A pixel gain variation frame, shown in Figure 12, is then applied to the data frames to yield the corrected data. This second order correction typically yields a factor of 3 to 10 additional noise reduction over flat fielding with conventional flat fields. A more detailed description of the algorithm and its application to the data has been given by Hammer, Peterson, and Smith (12).

The procedure is most effective when the pixel offset of the array is known or measurable, when fringe pattern variations are small between FPA rows and when the bad pixel density is low around the interferogram centerbursts. Ideally, a uniformly illuminated homogeneous target would yield the best results. The algorithm can be reformulated for treating non-linear dynamic range problems. It works best on systematic and spurious variations over the array that are proportional to the incident intensities. The algorithm is, however, not sensitive to modest deviations from the above conditions. Intensity variations over the spatial coordinate do not have adverse effects except when regions with

-8-

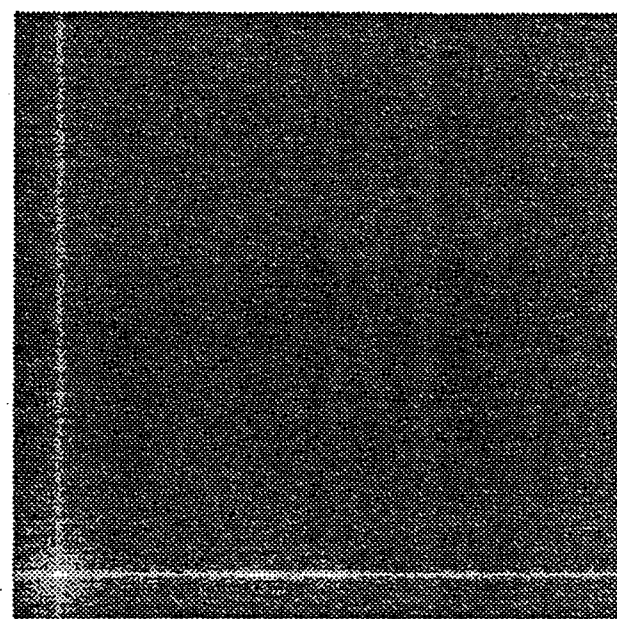
very low signal levels are present. Good results may even be attained if there is a moderate amount of spectral variability, as is the case for the example described above.

APPLICATIONS AND EXAMPLES

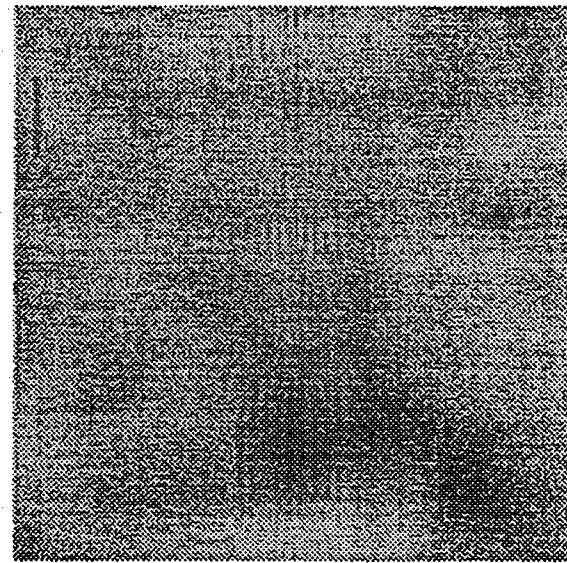
The effectiveness of the algorithm on measurement with the SWIR DASI is remarkable. The ingress part of the algorithm after the specified series of operations yields transformed data in the two-dimensional Fourier domain shown in Figure 12, where the bright lines represent the spectral frequency (horizontal) and spatial frequency coordinates with respect to the original DASI frame. The origin, which represents zero spatial and spectral frequencies, has been shifted from the edges of the frame to show the signal more clearly. A logarithmic intensity scale is used. The top and right edges correspond to the spatial and spectral Nyquist frequencies, respectively. The peak value of the spectrum (at about 6400 cm^{-1} spectral wavenumber and 0 spatial frequency - the bright region near the bottom and slightly left of center in Figure 12) is several hundred times higher than nearby points having non-zero spatial frequencies. The large contrast between the localized signal and the background makes this algorithm effective.

Signal-to-Noise Calculations From Actual Measurements

We configured the DASI initially at a spectral resolution of 60 nm at $1.5 \mu\text{m}$ with a free spectral range of over 10000 cm^{-1} . A typical terrestrial solar reflectance signal was observed. Within the $1.2 - 2.2 \mu\text{m}$ passband of the cold shortpass filter, there are 23 spectrally



2D FT of 100 coadded interferogram
frames after 1st order flat fielding
and fringe alignment



2nd order flat fielding frame

Figure 12. Upper panel demonstrates the algorithm's signal localization and lower panel shows the correction frame.

resolved channels, about half of which lie in atmospheric absorption bands. There are approximately twelve ($=N$) spectrally active channels. An array with 256 pixels along the interferogram coordinate (the fringes are oversampled) and photoelectron well depth of 3×10^5 electrons/pixel was used. The observing conditions are chosen so that these wells were 1/3 full on the average. Thus, there are $P = 2.6 \times 10^7$ total photoelectrons in the interferogram which from the relationship above predicts a signal-to-noise of about 400 per active spectral element.

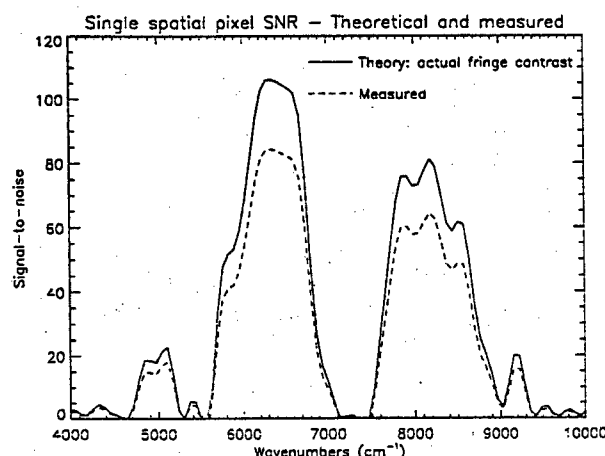


Figure 13. Signal-to-noise achieved compared with theoretical signal-to-noise.

Figure 13. shows single spatial pixel signal-to-noise ratios derived from a generalization of the above relationship accounting for the sensor line shape. A misalignment occurring during the flight, resulted in a fringe contrast of less than 40% while, typically, the fringe contrast is about 75-80%. The example for the measured SNR is derived from the hyperspectra described below after applying the flat-fielding algorithm to raw DASI data frames.

-10-

Observations from an airborne platform

During March 1994, about 30 DASI hyperspectra were acquired over coastal and inland regions of central California from the NASA C-130 aircraft with the DASI mounted over a nadir viewing port. An example of five selected planes from one hyperspectrum is shown in Figure 14. A swath covering agricultural fields with a NASA air strip diagonally across the upper left end is about 0.6 km by 3 km in area. The ground spatial resolution is about 2.4×31 meters, limited in the along track dimension by the 4 Hertz frame rate of the NICMOS III array.

The S/N in these data is high enough that detailed spectral analysis has proven useful. An analysis is underway and will be described in separate publications. A selection of spectra from pixels scattered across the area is shown in Figure 15 so as to provide some flavor of the spectral content. Atmospheric water and water contained in the plants is the strongest contributor to the spectral reflectance. Biological and mineralogical features are less prominent. There are numerous differences in the spectra of selected biological components. These components were catalogued in a ground-truth program. Segment 2, for example, contains the NASA tarmac and reveals a distinctive spectral reflectance compared with the surrounding vegetation. The spectral feature variations in the plotted spectra are a consequence of many factors including the particular vegetation observed, its state of development, the fraction of vegetative cover over the land and the soil characteristics. Qualitatively, the spectra are more similar within particular groups such

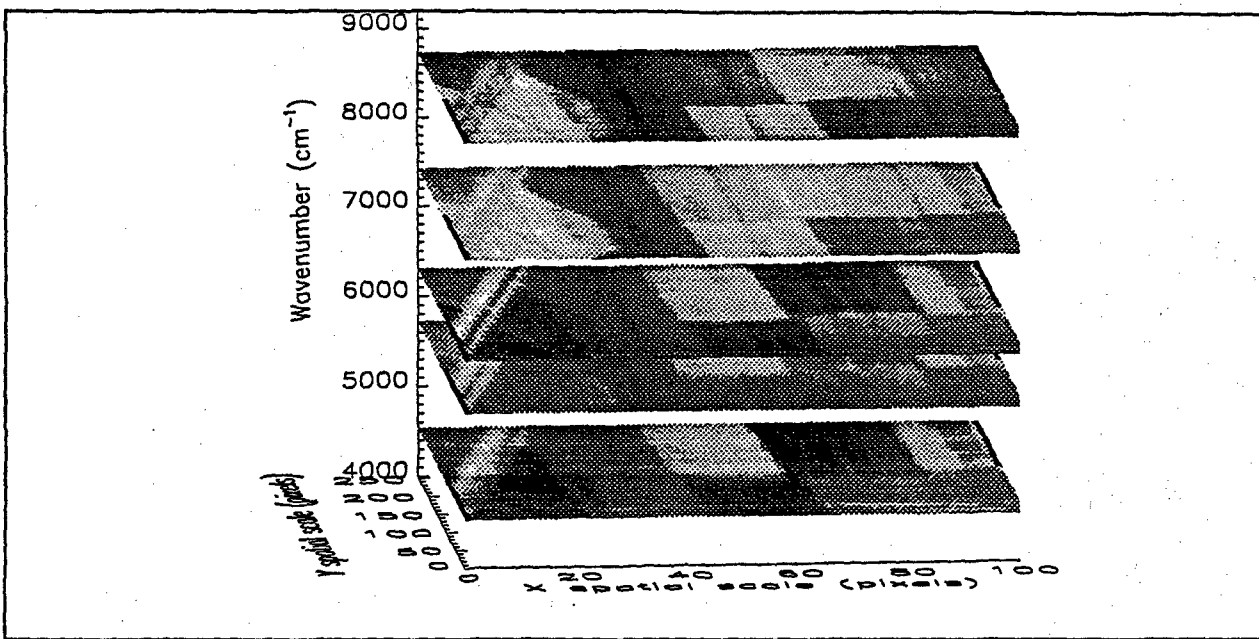


Figure 15. DASI hyperspectrum of agricultural fields and an air strip, showing five selected planes between 4300 and 8900 cm^{-1} .

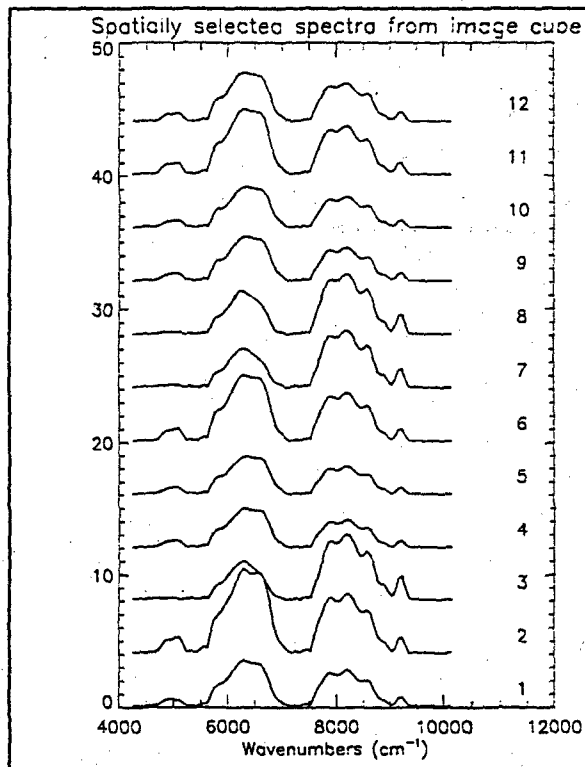


Figure 16. Selected individual spectra from fields and the tarmac hyperspectra.

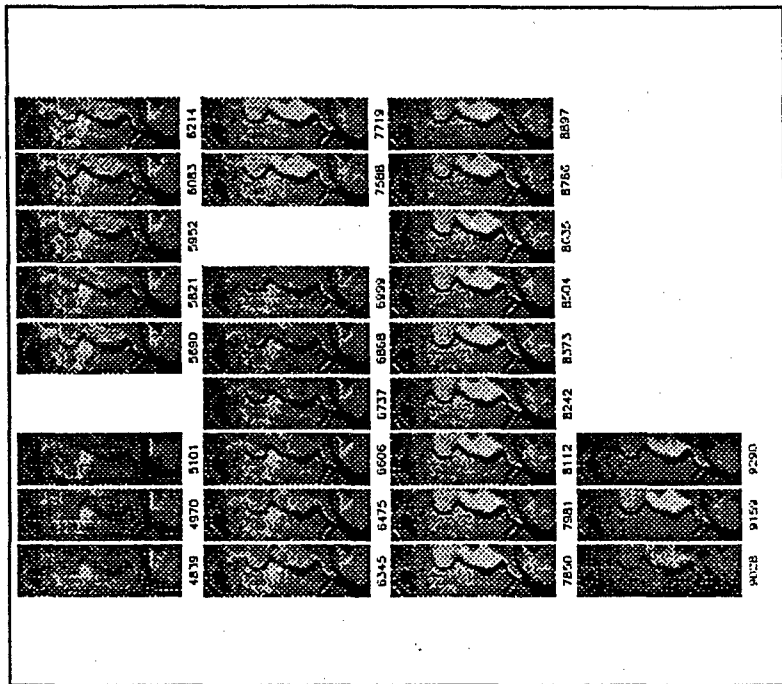


Figure 17. Spectral images at selected cm^{-1} where significant signal is observed. The interval between images is 113 cm^{-1} .



Figure 18. Spectral average DASI image, obtained during C130 flight east of Palo Alto, CA.

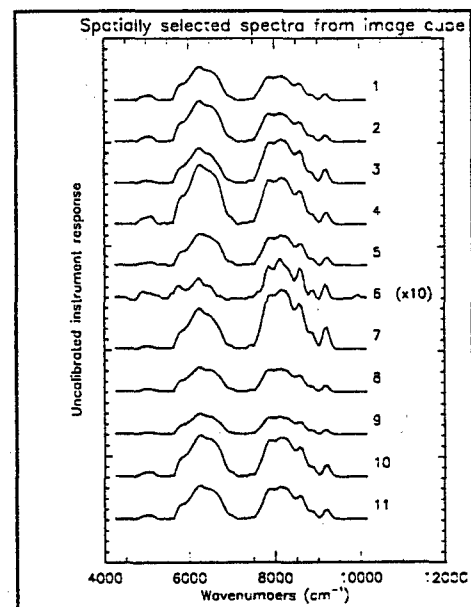


Figure 19. Spectra of numbered regions in Figure 18.

as beans and hay while the spectral differences between areas like hay or beans and the runway are readily evident.

SUMMARY

Specific DASI designs and certain properties are described and compared with dispersive and scanning FTS hyperspectral imagers. The field-widened capability is demonstrated from observational data. Measurements of Jupiter yield qualitatively typical spectra. Airborne observations of the Earth's land and water surface have been made using a prototype DASI. A novel flat-fielding algorithm has yielded a S/N performance with our present prototype DASI using CCDs and HgCdTe SWIR FPA that is photon-noise limited. These results support our theoretical analysis of anticipated S/N and encourage the application of DASIs to a variety of remote sensing applications.

ACKNOWLEDGMENTS

WHS acknowledges the support of NASA under its PIDDP program and under the Pluto Fast-Flyby Sensor Breadboard Program for their early support of the development of DASIs for planetary science missions. We acknowledge the continuing support of Dr. David Peterson for his encouragement in the application of the DASI concept to plant canopy studies. The Naval Research Laboratory has been supportive of DASI development for studies of littoral scenes.

The airborne measurements were made possible by flight time granted to us by NASA's Office of Mission to Planet Earth. Scott Hubbard, Roger Arno, and Marcus Murbach of the Space Projects office at NASA Ames and Gary Langford of SkyWatch, Inc. made substantial contributions to the DASI flight preparations and operations. Lee Johnson of Johnson Controls World Services at NASA Ames contributed to the site visits in support of the flight observations. We wish to express our appreciation to members of the C130 staff who helped us to interface our prototype sensor for its maiden flights.

REFERENCES

1. Stroke, G. W. and A. T. Funkhouser, "Fourier-Transform Spectroscopy Using Holographic Imaging without Computing and with Stationary Interferometers", *Phys. Letters*, 16, 272, (1965)
2. Yoshihara, K. and A. Kitade, "Holographic Spectra Using a Triangle Path Interferometer", *Japan. J. Appl. Phys.*, 6, 116, (1967)
3. Okamoto, T., S. Kawata and S. Minami, "A Photodiode Array Fourier Transform Spectrometer Based on a Birefringent Interferometer", *Appl. Spectrosc.*, 40, 691 (1986)
4. Douglas, N.G., Butcher, H.R., and Melis, W.A., *Astr. Space Sci.*, 171, 307, 1990.
5. Smith, W. H. and W. V. Schempp, "Digital Array Scanned Interferometers", *Exp. Astron.* 1, 389-405, 1991.
6. Smith, W. H., U.S. Patent No. 4,976,542, 1990.
7. Kahn, F. D., "The Signal: Noise Ratio of a Suggested Spectral Analyzer", *Ap. J.* 129, 518, (1959)
8. Brault, J., Kitt Peak National Observatory, "High Resolution Astronomy", Proc. 15th Advanced Course in Astronomy and Astrophysics, SaaFee, M. Huber, A. Benz, and M. Mayor, eds., 1985.
9. Jacquinot, P., "The Luminosity of Spectrometers with Prisms, Gratings, or Fabry-Perot Etalons", *J. Opt. Soc. Am.*, 44, 761, (1954)
10. Smith, W. H., Final Report on PRIMIS, Pluto Reflectance Imaging Interferometric Sensor (1995).

11. Bracewell, R., "The Fourier Transform and Its Applications", McGraw-Hill, 1965
12. Hammer, P. D., D. L. Peterson, and W. H. Smith. "Imaging interferometry for terrestrial remote sensing - Digital Array Scanned Interferometer instrument developments". In: Imaging Spectrometry, SPIE Aerospace Symposium, Proc. SPIE 2480, in press, 1995.
13. Forman, M. L., W. H. Steel, and G. A. Vanasse. "Correction of asymmetric interferograms obtained in Fourier spectroscopy", J. Opt. Soc. Am. 56, 59-63, 1966.
- Hammer, P. D., D. L. Peterson, and W. H. Smith. "An imaging interferometer for terrestrial remote sensing". In: Gregg Vane, Ed., Imaging Spectrometry of the Terrestrial Environment, Proc. SPIE 1937, 244-255, 1993.
- Hammer, P. D. and W. H. Smith. "Spectral imaging of clouds using a digital array scanned interferometer", Atmos. Res., 34, 347-366, 1994.
- Mertz, L., "Auxiliary computation for Fourier spectrometry", Infrared Phys. 7, 17-23, 1967.



Received 2/8/2000
DEPARTMENT OF THE ARMY
US ARMY MEDICAL RESEARCH AND MATERIEL COMMAND
504 SCOTT STREET
FORT DETRICK, MARYLAND 21702-5012

REPLY TO
ATTENTION OF:

MCMR-RMI-S (70-1y)

21 Jan 00

MEMORANDUM FOR Administrator, Defense Technical Information Center, ATTN: DTIC-OCA, 8725 John J. Kingman Road, Fort Belvoir, VA 22060-6218

SUBJECT: Request Change in Distribution Statement

1. The U.S. Army Medical Research and Materiel Command has reexamined the need for the limitation assigned to technical reports written for the attached Awards. Request the limited distribution statements for Accession Document Numbers listed be changed to "Approved for public release; distribution unlimited." These reports should be released to the National Technical Information Service.
2. Point of contact for this request is Ms. Virginia Miller at DSN 343-7327 or by email at virginia.miller@det.amedd.army.mil.

FOR THE COMMANDER:

Encl
as

Phylis Rinehart
PHYLIS M. RINEHART
Deputy Chief of Staff for
Information Management